

## Enhanced magnetoresistance and spin-filter effects in magnetic heterostructures

This article has been downloaded from IOPscience. Please scroll down to see the full text article.

2000 J. Phys.: Condens. Matter 12 L373

(<http://iopscience.iop.org/0953-8984/12/24/101>)

View [the table of contents for this issue](#), or go to the [journal homepage](#) for more

Download details:

IP Address: 171.66.16.221

The article was downloaded on 16/05/2010 at 05:12

Please note that [terms and conditions apply](#).

## LETTER TO THE EDITOR

**Enhanced magnetoresistance and spin-filter effects in magnetic heterostructures**M S Ferreira<sup>†</sup>, J d'Albuquerque e Castro<sup>†</sup>, R B Muniz<sup>†</sup> and Murielle Villeret<sup>‡</sup><sup>†</sup> Departamento de Física, Universidade Federal Fluminense, Niterói, Brazil<sup>‡</sup> Department of Mathematics, City University, London EC1V 0HB, UK

Received 25 April 2000

**Abstract.** We show that ballistic transport through a pair of superlatticed magnetic junctions connected by a low-density-of-carriers conducting medium can provide an efficient spin filter and cause an enhanced magnetoresistive response.

Spin-polarized transport in nano-structured systems has attracted much attention due to its importance in both basic research and technology [1]. The search for spin-filtering systems capable of producing currents of spin-polarized electrons is currently a focus of attention [2–5]. Systems showing high magnetoresistance are also of great interest in magnetics-based technology. In fact, the so-called giant-magnetoresistance (GMR) effect is currently being used by the magnetics industry in the development of devices such as ultra-sensitive magnetic field sensors, read heads, and random access memories. GMR is observed in structures made of alternating layers of ferromagnetic and non-magnetic materials. The effect consists of a substantial change in electrical resistance when an applied magnetic field changes the relative orientation of the magnetizations of the magnetic layers [6]. GMR is caused by spin-dependent scattering, and is detected as a response to currents flowing either in the planes (CIP) or perpendicularly to the planes (CPP) of the layers. The CPP geometry is the most suitable for fundamental studies because it may reduce the influence of impurity scattering. It also generally leads to higher MR ratios because the perpendicular current probes all layers on traversing the system. Practical sensors for magnetic recording require high MR for relatively low applied magnetic fields, typically less than a few oersteds.

Here we show that MR ratios several orders of magnitude higher than those previously observed can be obtained with superlatticed magnetic contacts separated by a current-carrying medium with a relatively low density of carriers. We also show that this type of structure can function as a spin filter in one of its magnetic configurations, and as an insulator in the reversed configuration. Such a transition from conducting to insulating is driven by an applied magnetic field that switches the magnetic configuration of the system, making it operate as a binary gate.

Our central idea is the use of the modulated character of the magnetic contacts to impose suitable spin-dependent boundary conditions on carriers in order to control the spin-polarized conductances across the structure. The principle is analogous to that described in reference [7], but used in reverse. We assume that the contacts are sufficiently small, and free of impurities, that the CPP transport occurs in the ballistic regime, and the conductance is obtained simply by counting the number of propagating states. In this case, the carrier motion separates

into components parallel and perpendicular to the superlattice modulation direction ( $\hat{z}$ ), with energies  $E_z$  and  $E_\perp$ , respectively.

Generally, the transmission across a superlatticed structure shows energy gaps, which result from quantum interferences due to reflections of the electronic wave function at the interfaces. The widths and positions of such gaps depend on the potential profile which describes the modulation of the heterostructure, i.e., on the heights and widths of the potential barriers felt by carriers as they travel across the structure. In magnetic superlattices, because of the exchange splitting in the ferromagnetic layers, the position and size of the gaps depend also on the relative orientation of the magnetizations of the magnetic layers, and may be very different for majority-spin ( $\uparrow$ ) and minority-spin ( $\downarrow$ ) carriers. For example, due to an almost perfect match between the minority-spin bands of Fe and Cr,  $\downarrow$ -spin electrons flowing across Fe/Cr superlattices are weakly scattered at the interfaces when the magnetic layers are ferromagnetically aligned. In contrast,  $\uparrow$ -spin electrons are strongly scattered in this configuration, leading to the appearance of transmission gaps. In fact, the projection of the majority-spin Fermi surface (FS) of Fe/Cr superlattices on a plane parallel to the layers shows several regions through which ballistic perpendicular currents cannot flow [8]. Such forbidden transmission channels play a very important role in the spin-polarized transport across those structures. In particular, when the Fermi level  $E_F$  lies in a transmission gap along  $\hat{z}$  for  $E_\perp = 0$ , the corresponding FS is open in this direction. The perpendicularly projected FS ( $FS_\perp$ ) then exhibits a hole, centred at the middle ( $\Gamma$  point) of the first Brillouin zone, representing a set of unavailable channels for ballistic perpendicular current carried by electrons with  $E_\perp$  below a certain value. Non-propagating states around  $\Gamma$  are relatively common, and can be found in various superlatticed structures [8, 9]. They occur, for example, in the projection of the majority-spin FS of a  $Fe_4/Cr_4$  (001)-oriented superlattice in the parallel configuration, and in the FS of either spin of a  $Co_5/Cu_5$  (001) multilayer in the antiparallel configuration [8]. Such a property, however, is not restricted to magnetic superlattices based on transition metals.

We examine a system made of two superlatticed magnetic layers separated by a non-magnetic spacer. Suppose the electrical current is injected and collected flowing along the modulation direction of the superlatticed contacts, as schematically represented in figure 1. Consider also that in a given magnetic configuration these superlattices exhibit a kind of  $\Gamma$ -centred hole in their  $FS_\perp$  for one spin direction, as previously described. If it occurs in the parallel configuration, the ferromagnetic superlatticed junctions must have different coercivities (which may be achieved by selecting them with different thicknesses), so that an applied magnetic field can switch the magnetization of one contact before that of the other to give the desired antiparallel alignment. Otherwise, the saturating field can be used to switch the magnetic configuration of both superlatticed contacts.



**Figure 1.** A schematic representation of the heterostructure showing the injector and collector magnetic superlattices, joined by a low-carrier-density spacer. The symbols  $\odot$  indicate the magnetization directions of the magnetic layers.

By considering non-magnetic spacers with low carrier densities, we see that the Fermi wave vector of the non-magnetic spacer can be smaller than a typical  $\Gamma$ -centred  $\text{FS}_\perp$  hole radius. In this case, the FS of the intervening medium fits entirely into the hole of the superlattice  $\text{FS}_\perp$ , and the transmission of carriers in one spin state is obstructed across the junctions. Thus, with a suitable choice of contacts and convenient number of carriers in the spacer, one can obtain a spin-polarized electrical current, and an enormous magnetoresistance with this type of heterostructure. To illustrate such an effect and the underlying physical mechanisms, we adopt a simple treatment in which both magnetic superlatticed contacts, and the spacer are described by free-electron models. Although the electronic structure of the magnetic contacts may be expressed in too-simple terms by such model, this description is sufficient to explain the main issues involved. We consider each superlatticed junction containing a finite number  $n_c$  of unit cells which are made of a magnetic layer  $M$  juxtaposed with a non-magnetic layer  $N$ , with thicknesses  $m$  and  $n$ , respectively. In order to analyse the ballistic CPP transport across such a structure, it is convenient to take the spin-quantization axis along the direction of the magnetization of the magnetic layers in both the parallel and antiparallel configurations. The electrical current then splits into  $\uparrow$ - and  $\downarrow$ -spin components which, in the absence of spin mixing, should be added in parallel. Along the CPP direction  $\hat{z}$ , carriers with spin  $\sigma$  experience a Kronig–Penney-like potential which equals either  $V^\uparrow$  or  $V^\downarrow$  inside a magnetic layer  $M$ , and  $V_N$  inside  $N$ ; perpendicularly to  $\hat{z}$  the carriers move freely. The spacer is characterized by a constant potential  $V_s$  which controls its density of carriers. The electrical conductances  $\Gamma^\sigma$  for carriers with spin  $\sigma$  depend on the magnetic configuration of the superlatticed junctions, because the potential profiles seen by carriers with different spin orientations change with the magnetic arrangement. As usual, the GMR ratio is defined by  $(\Gamma_{FM} - \Gamma_{AF})/\Gamma_{AF}$ , where  $\Gamma_{FM}$  and  $\Gamma_{AF}$  are the total conductances ( $\Gamma = \Gamma^\uparrow + \Gamma^\downarrow$ ) of the system in the ferromagnetic and antiferromagnetic configurations, respectively.

Within the Landauer–Büttiker formalism, the conductance at zero temperature is given by

$$\Gamma_{FM(AF)} = (e^2/h) \sum_{\vec{k}_\perp, \sigma} T_{FM(AF)}^\sigma(\vec{k}_\perp, E_F)$$

where  $T_{FM(AF)}^\sigma(\vec{k}_\perp, E_F)$  is the transmission coefficient of the system in the FM (AF) configuration for carriers with energy  $E_F$ , spin  $\sigma$ , and wave vector  $\vec{k}_\perp$  perpendicular to  $\hat{z}$ . In our model, the dependence on  $\vec{k}_\perp$  appears only via the energy component  $E_\perp = \hbar^2 k_\perp^2/2m$ ; therefore, it is possible to transform the summation over  $\vec{k}_\perp$  into an integral over  $E_\perp$ , and rewrite it as

$$\Gamma_{FM(AF)}^\sigma = (e^2/h) \int dE_\perp g(E_\perp) T_{FM(AF)}^\sigma(E_F - E_\perp)$$

where the integral extends up to  $E_F$ , and  $g(E_\perp)$  is the perpendicular density of states with energy  $E_\perp$ . For each value of  $E_\perp$ , the transmission coefficients  $T^\sigma$  are obtained by solving an effective one-dimensional quantum-mechanical problem [7].

We consider superlatticed junctions of different thicknesses, with  $n_c^i$  and  $n_c^c$  cells for the injector and collector, respectively. In order to reduce the number of variables in the model, we assume perfect matching between  $V^\downarrow$  and  $V_N$ , so  $\downarrow$ -spin carriers experience no change in their local potentials when they move across the magnetic superlattice interfaces.  $V^\uparrow$ ,  $m$ ,  $n$ , and  $E_F$  are chosen to ensure that the magnetic superlattice has a  $\Gamma$ -centred hole in its  $\uparrow$ -spin  $\text{FS}_\perp$ . The contacts are placed a certain distance apart, so that  $V_s$  has length  $L$ . First we examine the ferromagnetic configuration, and look at the transmission curves  $T_{FM}^\uparrow(E)$ , as functions of  $E$ , for two different values of  $V_s$ . The results are presented in figure 2. In our calculations we have used  $m = n = 5$ ,  $n_c^i = 20$ ,  $n_c^c = 30$ ,  $V_\uparrow = -0.08$ ,  $V_\downarrow = V_N = 0$ , and  $L = 20$ . Here,

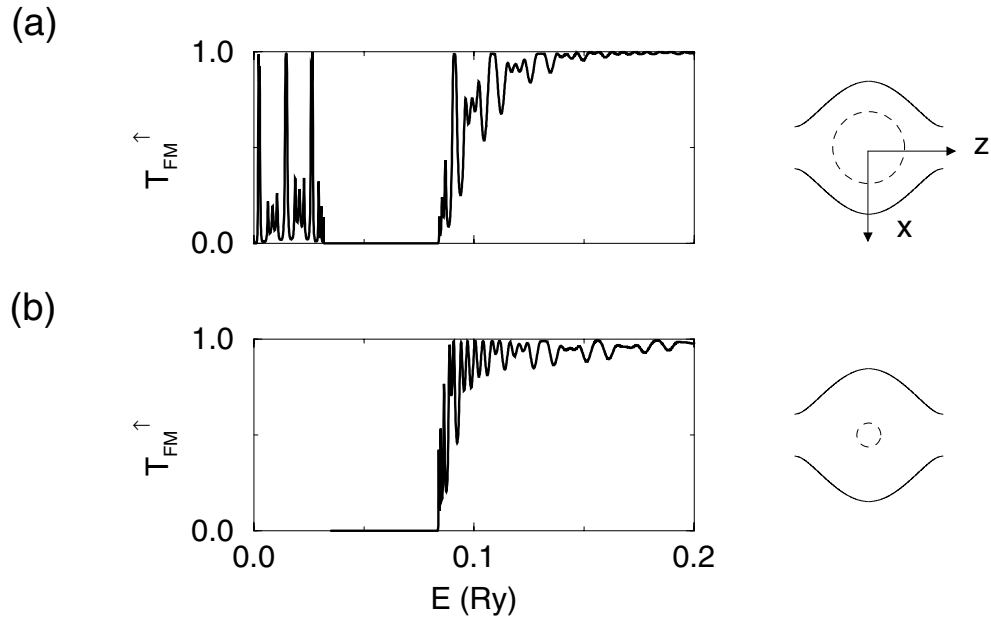


**Figure 2.** Transmission coefficients  $T_{FM}^{\uparrow}$ , calculated as functions of energy, for  $V_s = 0$  (a) and  $V_s = 0.035$  (b). The other potential parameters are defined in the text. On the right-hand side we show schematic representations of the corresponding bulk Fermi contours of the magnetic superlattice (solid line) and of the low-carrier-density intervening medium (dashed lines).

energies and lengths are measured in atomic units. Although the electronic effective mass  $m$  may vary along  $\hat{z}$  for some cases of interest, we have assumed, for simplicity, a constant value  $m = 1$  in our calculations.

The transmission coefficient  $T_{FM}^{\uparrow}(E)$ , calculated for  $V_s = 0$ , is shown in figure 2(a), and it clearly exhibits a gap which is preceded by a transmission band. The gap comes from the superlatticed structure of the junctions, and the transmission band indicates the existence of available conducting channels for carriers with energies below the gap. For a fixed value of  $E_F$  the density of carriers in the spacer decreases as  $V_s$  increases. It is evident from figure 2(b) that the transmission band below the gap is totally suppressed for  $V_s = 0.035$ . As mentioned earlier, for values of  $E_F$  within the gap, the  $\uparrow$ -spin bulk FS of the magnetic superlattice is open along  $\hat{z}$ , and its projection has a hole at the centre of the first BZ. For an intervening medium with sufficiently low density of carriers,  $V_s$  is close to  $E_F$ , and the spacer FS is so small that it lies entirely within the  $\Gamma$ -centred hole of the magnetic superlattice FS. This is schematically illustrated on the right-hand side of figure 2, where a cross-section of the bulk Fermi surface of the corresponding magnetic superlatticed structure (full line) and of the spacer (dashed line) are shown.

In the calculations of conductances  $\Gamma^{\sigma}$ , the corresponding transmission coefficients are integrated over energy up to  $E_F$ . Therefore, the presence of a transmission band below the Fermi energy in  $T^{\sigma}$  leads to a non-vanishing value of  $\Gamma^{\sigma}$ . Hence, for  $E_F = 0.08$  and  $V_s = 0$ , both  $\Gamma_{FM}$  and  $\Gamma_{AF}$  are non-zero, and an ordinary GMR effect is obtained. It is noteworthy that if we assume perfect matching between  $V_{\downarrow}$  and  $V_N$ , there will be no gaps in  $T_{FM}^{\downarrow}$ . For  $V_s = 0.035$ , however, all transmission vanishes for  $E < E_F$ , except  $T_{FM}^{\downarrow}$  which has no gaps. Both spin channels are blocked in the AF configuration due to the antiparallel alignment of the contact magnetizations. Thus, all conductances but  $\Gamma_{FM}^{\downarrow}$  vanish (i.e.,  $\Gamma_{AF} \approx 0$  and

$\Gamma_{FM} \approx \Gamma_{FM}^\uparrow$ ), because the conducting channels in the intervening medium have no counterpart in the superlatticed junctions, and vice versa. In this case, the system behaves as a spin-filter conductor in the FM configuration, and as an insulator in the AF one, thereby exhibiting an infinitely large MR ratio<sup>†</sup>. It is worth mentioning that for finite values of  $n_c^i$  and  $n_c^c$ , quantum tunnelling across the junctions leads to a non-zero transmission in the gap region, but such tunnelling vanishes rapidly as  $n_c^i$  and  $n_c^c$  increase. The enhanced MR effect is depicted in figure 3(d), and in figures 3(a), 3(b), and 3(c) we show the corresponding partial conductances  $\Gamma_{FM}^\uparrow$ ,  $\Gamma_{FM}^\downarrow$ , and  $\Gamma_{AF}^\uparrow$ , calculated as functions of  $V_s$ , for the same set of parameters as listed above. We omit the curve for  $\Gamma_{AF}^\downarrow$  because it is very similar to that of  $\Gamma_{AF}^\uparrow$  (they are not identical because  $n_c^i \neq n_c^c$ ). One clearly sees that as soon as  $V_s$  reaches the lower energy gap boundary, it suppresses the transmission band below  $E_F$  in  $T_{FM}^\uparrow$ , and all conductances but  $\Gamma_{FM}^\uparrow$  become vanishingly small.

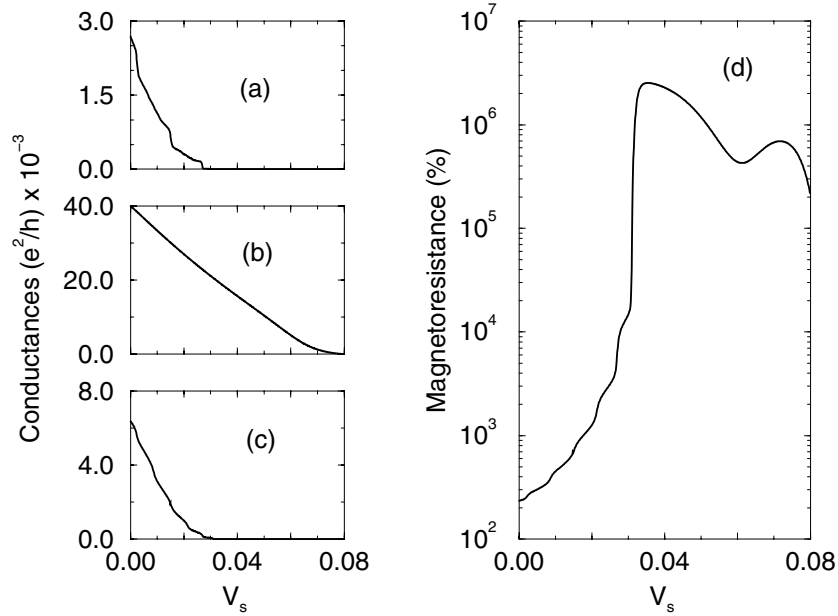


**Figure 3.** Partial conductances  $\Gamma_{FM}^\uparrow$  (a),  $\Gamma_{FM}^\downarrow$  (b), and  $\Gamma_{AF}^\uparrow$  (c), as well as a magnetoresistance ratio (d), as functions of  $V_s$  (see the text).

In conclusion, we have shown that by using a heterostructure made of magnetic superlatticed junctions separated by a low-carrier-density medium, it is theoretically possible to obtain an enhanced magnetoresistance response several orders of magnitude larger than ordinary GMR. This enhanced GMR effect is based on the existence of spin-dependent transmission gaps caused by the superlatticed structure of the magnetic contacts, which selectively obstructs the propagation of carriers in one spin state across the structure. The ability to manipulate the gaps by varying the modulation of superlatticed structures, and by tuning the density of carriers in the spacer, enables control of the spin-polarized transport through these systems. The insulating-to-conducting transition driven by the applied magnetic field that causes this effect introduces an extra advantage for the ballistic CPP measurements. One of the difficulties encountered in measuring MR in the CPP geometry is that the resistances involved

<sup>†</sup> Here ‘AF configuration’ stands for the situation in which the magnetizations of the injector and collector are anti-aligned, not for each superlatticed junction being in an AF configuration.

are very small. One way of circumventing this problem is to reduce the cross-sectional area of the sample by micro-lithography. Here we can exploit the voltmeter apparatus limitations and adjust the heterostructure in such a way that it acts as a binary gate, or high-pass current filter, where only the resistance for a given magnetic configuration is sufficiently large to be detected.

The effect reported here relies on transport taking place within the ballistic regime. Therefore, in practice, interfacial inhomogeneities should be avoided, because they destroy in-plane wave-vector conservation and mix the transmission channels, thereby spoiling the gap and reducing the magnetoresistance enhancement. Preliminary calculations for two-dimensional systems show that the effect is substantially reduced by the presence of impurities at the interfaces. However, in the dilute limit, it is rather robust, and still leads to MR responses orders of magnitude larger than conventional GMR. From the experimental point of view it may be difficult to completely avoid interfacial inhomogeneities, but recent advances in multilayer growth techniques and precise control in the deposition process have produced epitaxial growth of certain multilayers with virtually no layer fluctuations over macroscopic distances [10, 11].

Finally, it is worth pointing out that although we have illustrated the effect with metallic materials in mind, this is by no means a necessary requirement for the realization of the effect. Semiconducting materials such as those recently used for electrical spin injection [12, 13] may display such properties. As long as the magnetic superlatticed junctions exhibit a kind of  $\Gamma$ -centred hole in their  $FS_{\perp}$  for one spin direction, and the intervening current-carrying medium has a sufficiently low density of carriers, the CPP ballistic transport across the combined structure can show a huge MR effect.

Financial support from CNPq and FAPERJ (Brazil), the Brazilian Academy of Science and the Royal Society (UK) is gratefully acknowledged

## References

- [1] Prinz G A 1998 *Science* **282** 1660  
Prinz G A 1995 *Phys. Today* **48** (April) 58
- [2] Kane B E 1998 *Nature* **393** 133
- [3] DiVincenzo D P 1998 *Nature* **393** 113
- [4] Gardelis S, Smith C G, Barnes C H W, Linfield E H and Ritchie D A 1999 *Phys. Rev. B* **60** 7764  
Lee W E, Gardelis S, Choi B-C, Xu Y B, Smith C G, Barnes C H W, Ritchie D A, Linfield E H and Bland J A C 1999 *J. Appl. Phys.* **85** 6682
- [5] Hammar P R, Bennett B R, Yang M J and Johnson M 1999 *Phys. Rev. Lett.* **83** 203  
Datta S and Das B 1990 *Appl. Phys. Lett.* **56** 665
- [6] Baibich M N *et al* 1988 *Phys. Rev. Lett.* **61** 2472
- [7] Ferreira M S, d'Albuquerque e Castro J, Muniz R B and Villeret M A 1999 *Appl. Phys. Lett.* **75** 2307  
Ferreira M S, d'Albuquerque e Castro J, Muniz R B and Villeret M A 2000 *J. Phys.: Condens. Matter* **12** 2833
- [8] Schep K M, Kelly P J and Bauer G E W 1998 *Phys. Rev. B* **57** 8907 and references therein
- [9] López Sancho M P, Chico L and Muñoz M C 1999 *Phys. Rev. B* **59** 1232
- [10] Paggel J J, Miller T and Chiang T-C 1998 *Phys. Rev. Lett.* **81** 5632
- [11] Unguris J, Celotta R J and Pierce D T 1997 *Phys. Rev. Lett.* **79** 2734
- [12] Fiederling R, Kelm M, Reuscher G, Ossau W, Schmidt G, Waag A and Molenkamp L W 1999 *Nature* **402** 787
- [13] Ohno Y, Young D K, Beschoten B, Matsukura F, Ohno H and Awschalom D D 1999 *Nature* **402** 790